Theoretical and numerical analyses for PDM-IM signals using Stokes vector receivers

Jiahao HUO[1,2], Xian ZHOU[1,2*], Chao SHANG[3], Wei HUANGFU[1], Jinhui YUAN[1], Huansheng NING[1], Keping LONG[1], Changyuan YU[2], Alan Pak Tao LAU[4] & Chao LU[2]

[1]*Beijing Engineering and Technology Research Center for Convergence Networks and Ubiquitous Services, University of Science and Technology Beijing, Beijing* 100083, *China;*
[2]*Department of Electronic and Information Engineering, The Hong Kong Polytechnic University, Hong Kong* 999077, *China;*
[3]*Key Laboratory of Luminescence and Optical Information, Ministry of Education, Institute of Optical Information, School of Science, Beijing Jiaotong University, Beijing* 100044, *China;*
[4]*Department of Electrical Engineering, The Hong Kong Polytechnic University, Hong Kong* 999077, *China*

Abstract Different from current coherent-detection-based long-haul transmission systems, inter- and intra-datacenter transmissions require a simpler transmitter and receiver. A promising way to significantly meet the demands of datacenter transmission is polarization division multiplexing intensity modulation with direct detection (PDM-IM-DD) using a Stokes vector receiver (SVR). However, for different SVR architectures, the corresponding demultiplexing matrix is required to recover the Stokes vectors from the detected signals, which are combined with an arbitrary state of polarization (SOP), will change the effect of noise dynamically and significantly influence the system performance. In this study, PDM-IM signals using four SVRs, i.e., a 90° optical hybrid with 2 balanced photodetectors (BPDs) and 2 photodetectors (PDs), a 90° optical hybrid with 4 PDs, a Stokes analyzer and a 3 × 3 coupler with 4 PDs, are studied theoretically and numerically. Theoretical system models using the four SVRs are developed, and the noise power variations are analyzed quantitatively based on these models. Moreover, the performance of the systems is also investigated for 224 Gbit/s polarization division multiplexing pulse amplitude modulation 4 level with direct detection (PDM-PAM4-DD) transmission in a simulation. The simulation results show that the bit error rate (BER) performance of the systems is consistent with the theoretical noise power variation curves. The theoretical analysis scheme is helpful for the practical design of SVR-based systems.

Keywords short-reach optical communications, PAM4, polarization division multiplexing, Stokes vector, direct detection

1 Introduction

Recently, most popular Internet applications operate in a datacenter infrastructure, including cloud computing, storage, the Internet of Things (IoT), and other advanced applications. Datacenter networks, including intra- and inter-datacenter transmissions, typically range from a few meters to a few tens of kilometers [1–3]. Unlike traditional long-haul transmission, polarization division multiplexing with coherent detection (PDM-CO) schemes provides 4 degrees (4D) of freedom, including optical intensity, phase, and polarization. The use of in-phase and quadrature (IQ) modulators and a receiver local

* Corresponding author (email: zhouxian219@ustb.edu.cn)

oscillator increases the system cost and transceiver footprint [4, 5]. Complicated coherent detection digital signal processing (DSP) algorithms will also increase the power consumption. However, low cost and low power consumption are stringent requirements for datacenter networks. Intensity modulation with direct detection (IM-DD) based optical interconnects has become the technology of choice to scale DC networks because they are technologically simple and cost-effective and have small form factors [6,7]. However, standard IM-DD systems only support 1D of freedom. Here, to increase the capacity of IM-DD systems, one way is to use advanced modulation formats, including pulse amplitude modulation (PAM) [8–10], discrete multitone (DMT) modulation [11,12] and carrier-less amplitude, and phase (CAP) modulation [13]. Among these three advanced modulation formats, PAM is the simplest to implement. In particular, PAM4 has been selected as the most cost-effective solution for next-generation 400 GE [14].

Polarization division multiplexing with direct detection (PDM-DD) aims to utilize the polarization state of the signal to further enhance the capacity. Nevertheless, the application of PDM in IM-DD systems lags far behind PDM-CO systems, because PDM-DD systems hardly recover the full 4D information in the Jones space. In addition to the Jones space, the Stokes space expresses the state of polarization (SOP) in terms of optical power, which is more suitable for PDM-DD systems. In recent years, several Stokes vector receivers (SVRs) have been exploited for modulations ranging from 2D to 4D [15–21]. Morsy-Osman et al. [15] reported a 90° optical hybrid with 2 balanced photodetectors (BPDs) and 2 photodetectors (PDs) based SVR. Kikuchi et al. [16] proposed a receiver based on a Stokes analyzer. Shieh et al. [17] proposed an SVR based on a 3 × 3 coupler. These SVRs have a unique mapping matrix to recover the Stokes vectors. However, for a modulation above 2D in these SVRs, a transmitter electrical-field modulation or complex receiver architecture is required. Although these systems have the advantage of high capacity, the complex transceiver or DSP might not be cost- and power-effective [18]. Therefore, 2D-based PDM-PAM4-DD systems are the most attractive solution in datacenter networks. For the above SVRs, we noticed that the noise characteristics of the SVRs have not yet been studied.

In this paper, we focus on a theoretical analysis of polarization division multiplexing intensity modulation (PDM-IM) signals in different SVR architectures, i.e., a 90° optical hybrid with 2 BPDs and 2 PDs, a 90° optical hybrid with 4 PDs, a Stokes analyzer and a 3 × 3 coupler with 4 PDs. We develop the PD thermal noise for PDM-IM-DD systems in which Gaussian noise is dominant. Here, the noise varies during the Stokes vector recovery for different SOPs and SVRs. We fairly evaluate these four SVRs via the PD thermal noise. The relationship between the SOP and the PD thermal noise is studied in numerical simulations. To verify the theoretical analyses, a 224 Gbit/s PDM-PAM4-DD simulation setup is demonstrated. The bit error rate (BER) performance for different SOPs is analyzed by using the normalized noise power. The simulation results show that the BER performance of the systems is consistent with the theoretical noise power variation curves.

2 Principle of Stokes vector receivers

Conventionally, there are two polarization components in standard single-mode fiber (SSMF). The optical PDM signals can be described in the Jones space by separately describing the electric field vector of the X and Y components:

$$E = \begin{bmatrix} E_x \\ E_y \end{bmatrix}, \tag{1}$$

where E_x and E_y denote the electric fields of the X and Y polarization, respectively.

After fiber transmission, the SOP of the transmitted signal $s(t)$ will be changed randomly. The generalized description of the SOP rotation can be described by using a two-by-two Jones matrix [22,23]. When only the polarization rotation is taken into account in the SSMF, the received electric fields of the PDM signals, i.e., $E_{r,x}(t)$ and $E_{r,y}(t)$, can be obtained as

$$\begin{bmatrix} E_{r,x}(t) \\ E_{r,y}(t) \end{bmatrix} = \begin{bmatrix} \mathrm{e}^{\mathrm{j}\varepsilon}\cos\theta & -\mathrm{e}^{-\mathrm{j}\varepsilon}\sin\theta \\ \mathrm{e}^{\mathrm{j}\varepsilon}\sin\theta & \mathrm{e}^{-\mathrm{j}\varepsilon}\cos\theta \end{bmatrix} \cdot \begin{bmatrix} E_{t,x}(t) \\ E_{t,y}(t) \end{bmatrix}, \tag{2}$$

where θ and ε denote the random rotation angle and azimuth angle, respectively. The vectors denoting the complex envelope are also known as the Jones vectors.

In addition to the Jones space, another SOP representation of an optical signal is the Stokes space, which expresses the SOP in terms of optical power. The four Stokes vectors are

$$\begin{aligned} S_0 &= |E_x|^2 + |E_y|^2, \quad S_2 = 2\,\mathrm{Re}\left\{E_x E_y^*\right\}, \\ S_1 &= |E_x|^2 - |E_y|^2, \quad S_3 = 2\,\mathrm{Im}\left\{E_x E_y^*\right\}, \end{aligned} \tag{3}$$

and $S_0 = \sqrt{S_1^2 + S_2^2 + S_3^2}$. With a polarization rotation, the received Stokes vectors are given by

$$\begin{bmatrix} S_{r,0} \\ S_{r,1} \\ S_{r,2} \\ S_{r,3} \end{bmatrix} = \begin{bmatrix} 1 & 0 & 0 & 0 \\ 0 & \cos 2\theta & -\sin 2\theta \cos 2\varepsilon & \sin 2\theta \sin 2\varepsilon \\ 0 & \sin 2\theta & \cos 2\theta \cos 2\varepsilon & -\cos 2\theta \sin 2\varepsilon \\ 0 & 0 & \sin 2\varepsilon & \cos 2\varepsilon \end{bmatrix} \begin{bmatrix} S_{t,0} \\ S_{t,1} \\ S_{t,2} \\ S_{t,3} \end{bmatrix}. \tag{4}$$

The Stokes vectors include four components, $|E_x|^2$, $|E_y|^2$, $\mathrm{Re}\left\{E_x E_y^*\right\}$ and $\mathrm{Im}\left\{E_x E_y^*\right\}$, which contain 3D of freedom, i.e., the signal power in the X and Y polarization and the phase difference in inter-polarization. Therefore, in principle, it can construct a Stokes vector space direct detection (SV-DD) receiver to support 2D or 3D modulation and dramatically increase the overall transmission capacity. In 2D transmission systems, we use a PDM-IM transmitter. The transmitter sends two IM signals with orthogonal polarization. The two IM signals are contained in S_0 and S_1. Typical SVR structures are shown in Figures 1(a)–(d). For receiver A, the optical signal is split into two orthogonal polarization after the polarization beam splitter (PBS). Then, the two separated signals are sent into two 2×2 polarization-maintaining couplers. The coupler ratio is γ. The Stokes parameters $S_{r,0}$ and $S_{r,1}$ are obtained by the single PDs. $S_{r,2}$ and $S_{r,3}$ are obtained by 90° hybrid and BPDs. Considered 90° hybrid 1.2 dB insertion loss (IL) and 2×2 coupler 0.15 dB IL, when 2×2 coupler ratio is 0.7, the receiver gives the Stokes parameters' coefficients which readily have the proper scaling factors of the Stokes parameters. This guarantees that the performance will be SOP independent. Here, we investigate $\gamma = 0.5$ (normal case) and $\gamma = 0.7$ (SOP-independent case). After the 90° optical hybrid, the four outputs can be detected by 2 BPDs and 2 PDs. Receiver B in Figure 1(b) is a simplified solution. 2 PDs are employed instead of 2 BPDs at the outputs of the 90° optical hybrid. Figure 1(c) shows a Stokes analyzer receiver. Figure 1(d) shows an SVR based on a 3×3 coupler [17].

In each SVR, we define four branch output currents as $I = [I_1, I_2, I_3, I_4]^{\mathrm{T}} + N$, where $N = (n_1, n_2, n_3, n_4)$ denotes the receiver noise. Here, we assume that the system is dominated by Gaussian-like thermal noise. By using a 4×4 mapping matrix M, the receiver-side Stokes vectors can be obtained as $S_{r,0,1,2,3} = MI$. For the four different SVRs, the mapping matrices M are given as follows:

$$\begin{aligned} M_a &= \begin{bmatrix} \frac{1}{(1-\gamma)} & 0 & 0 & \frac{1}{(1-\gamma)} \\ \frac{1}{(1-\gamma)} & 0 & 0 & -\frac{1}{(1-\gamma)} \\ 0 & \frac{2}{\gamma} & 0 & 0 \\ 0 & 0 & \frac{2}{\gamma} & 0 \end{bmatrix}, \qquad M_b = \begin{bmatrix} \frac{1}{(1-\gamma)} & 0 & 0 & \frac{1}{(1-\gamma)} \\ \frac{1}{(1-\gamma)} & 0 & 0 & -\frac{1}{(1-\gamma)} \\ -\frac{1}{(1-\gamma)} & \frac{4}{\gamma} & 0 & -\frac{1}{(1-\gamma)} \\ -\frac{1}{(1-\gamma)} & 0 & \frac{4}{\gamma} & -\frac{1}{(1-\gamma)} \end{bmatrix}, \\ M_c &= \begin{bmatrix} \frac{1}{(1-\gamma)} & 0 & 0 & 0 \\ -\frac{1}{(1-\gamma)} & \frac{2}{(1-\gamma)} & 0 & 0 \\ -\frac{1}{(1-\gamma)} & 0 & \frac{2}{(1-\gamma)} & 0 \\ -\frac{1}{(1-\gamma)} & 0 & 0 & \frac{2}{(1-\gamma)} \end{bmatrix}, \; M_d = \begin{bmatrix} 1 & 1 & 1 & 1 \\ \frac{2}{1-\gamma} - 1 & -1 & -1 & -1 \\ 0 & -\sqrt{\frac{3}{\gamma}} & 0 & \sqrt{\frac{3}{\gamma}} \\ 0 & \frac{1}{\sqrt{\gamma}} & -\frac{1}{\sqrt{\gamma}} & \frac{2}{\sqrt{\gamma}} \end{bmatrix}, \end{aligned} \tag{5}$$

where M_a, M_b, M_c and M_d are the mapping matrices. S_R is calculated by using mapping matrices and the output I. During the S_R calculation, the relative noise is also mapping into the Stoke space as $N_S = MN$. In the Stokes space, the transfer function is expressed as

$$S_R = HS_T + N_S, \tag{6}$$

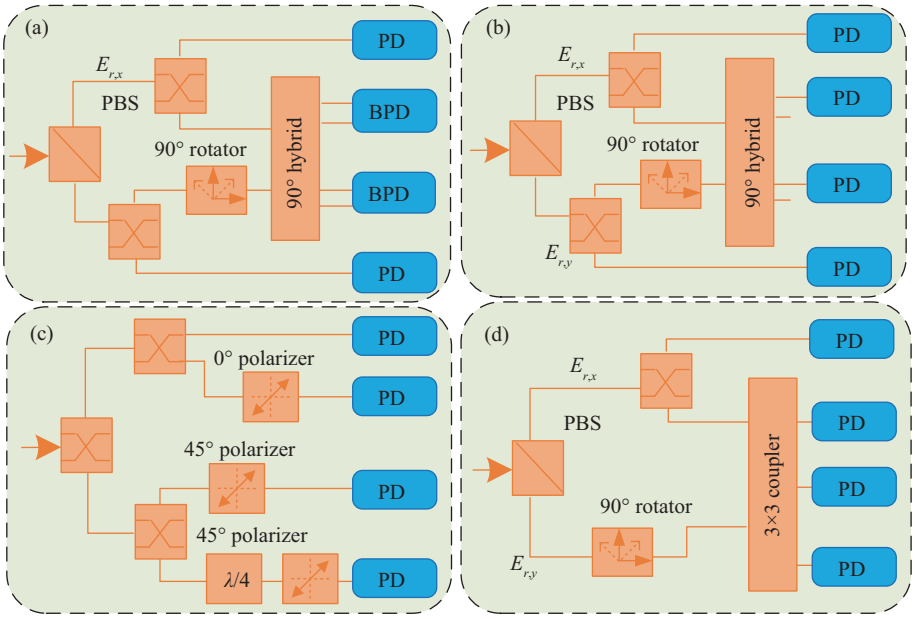

Figure 1 (Color online) Structures of the SVRs. (a) Receiver A: 90° optical hybrid with 2 BPDs and 2 PDs. (b) Receiver B: 90° optical hybrid with 4 PDs. (c) Receiver C: Stokes analyzer. (d) Receiver D: 3 × 3 coupler with 4 PDs.

where S_T is the transmitter side SV, N_S is an additive Gaussian noise and H is the channel matrix. For simplicity, we only consider the random polarization rotation in the following theoretical analysis (Eq. (4)). The optical channel usually varies on the time scale of a millisecond, and the channel matrix H can be obtained by pilot-aided or blind channel estimation [15, 16]. $\tilde{S}_T$ can be estimated by reversing the channel matrix:

$$\tilde{S}_T = H^{-1}HS_T + H^{-1}N_S = S_T + \tilde{N}, \tag{7}$$

where $(\cdot)^{-1}$ denotes the inverse of a matrix, because the noise vector $\tilde{N}$ undergoes the same transformation process, it can be written as

$$\tilde{N} = H^{-1}N_S = H^{-1}MN. \tag{8}$$

We can see from (8), the noise power changes with the SOP rotation. For the different SVR systems shown in Figure 1, $S_{t,0}$ and $S_{t,1}$ contain the intensity information of the two polarization. $\tilde{n}_1$ and $\tilde{n}_2$ are the noise of $\tilde{S}_{T0}$ and $\tilde{S}_{T1}$, respectively. So, in PDM-IM-DD systems, $\tilde{n}_1$ and $\tilde{n}_2$ are the dominant noise. Figure 2 shows the normalized noise power as a function of the received SOPs of PDM-IM signals in different SVRs by theoretical calculation.

Here, we scanned the rotation angle and azimuth angle from 0° to 180°. The SVRs encounter unequal noise power at different rotation angles. In view of Figure 2, the fundamental reason for the noise fluctuation at different SOP states is the lack of optical power (and hence lower signal-to-noise ratio). When the receiver thermal noise is added to signals provided by the optical front-end, the relative difference in optical power among the branches impacts the signal-to-noise ratio the most when SOP is rotated. For receiver A, as shown in Figure 2(a), when the 2 × 2 coupler ratio is $\gamma = 0.5$ in the normal case, the minimum noise power appears at $\theta = 0°, 90°, 180°$, and the maximum noise power appears at $\theta = 45°, 135°$. The difference between the maximum and minimum noise power is 4 dB. When the 2 × 2 coupler ratio is $\gamma = 0.7$, the noise power is flatter than when $\gamma = 0.5$, but the overall noise power is high. For receiver B, 2 PDs are employed instead of 2 BPDs. The system cost is lower than that of receiver A, but the difference between the maximum and minimum noise power is large at 7 dB. For receiver C, the noise power floor is high because of the large penalty in the mapping matrix. For receiver D, the noise power is independent of the SOP, and the noise power is lowest among the four receivers.

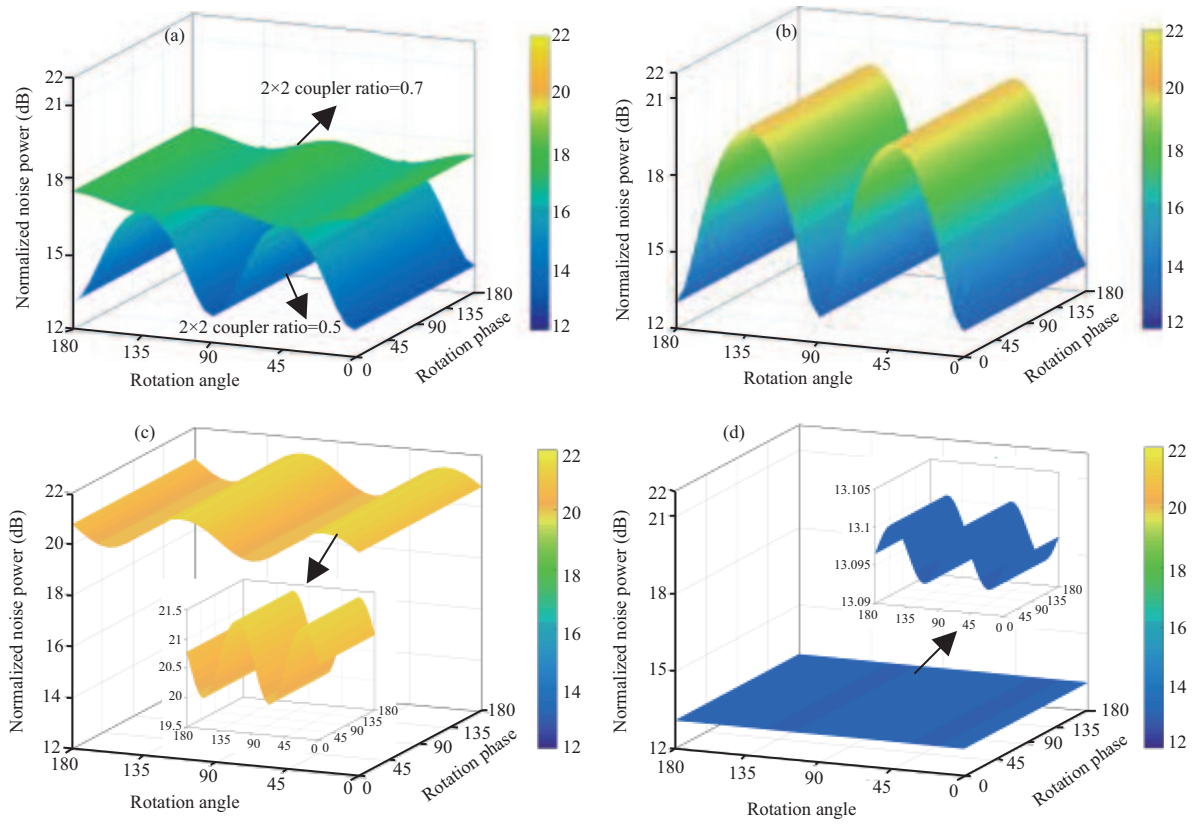

Figure 2 (Color online) Normalized noise power vs. the SOP rotation angle of PDM-IM signals in different SVRs. (a) Receiver A, (b) receiver B, (c) receiver C and (d) receiver D.

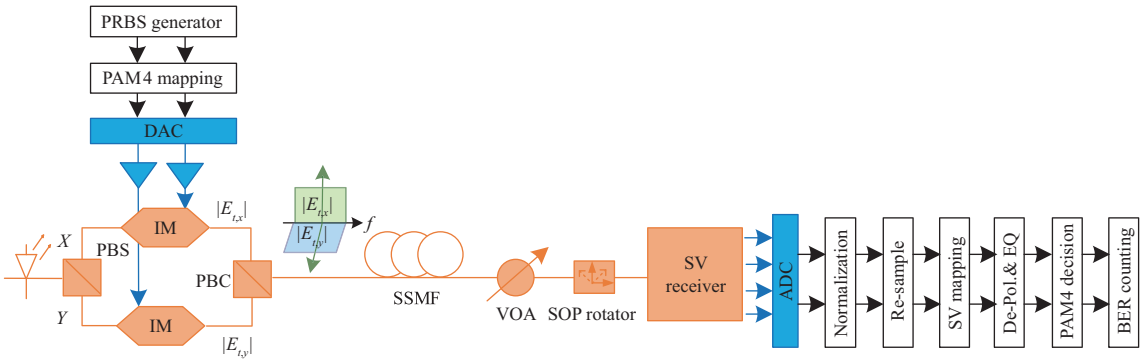

Figure 3 (Color online) Simulation setup for the 224 Gbit/s PDM-PAM4-DD system. PBS: polarization beam splitter. IM: intensity modulator. PBC: polarization beam combiner. SSMF: standard single-mode fiber. VOA: variable optical attenuator.

3 Simulation setup and results

Intra- and inter-datacenter transmission links with a few kilometers connect one datacenter to another. On one hand, owing to the intermodal dispersion in this length scale, SSMF is more suitable than multimode fiber (MMF). On the other hand, optical amplifiers are not preferred which length scale is still short. So, the receiver sensitivity is an important parameter for the system performance.

The simulation setup for the PDM-PAM4-DD systems is developed by VPI Transmission Maker 8.7 and MATLAB software, as shown in Figure 3. At the transmitter side, a pseudorandom binary sequence (PRBS) with a length of $2^{16} - 1$ is mapped into the PAM4 format. Then, the digital PAM4 signal is uploaded into a digital-to-analog converter (DAC). Two 56 Gbaud PAM4 signals are modulated onto

Table 1 General simulation parameters of 224 Gbit/s PDM-PAM4-DD systems

Parameter	Value	Parameter	Value
Wavelength	1310 nm	Laser Linewidth	10 MHz
DAC/ADC resolution	8 bit	Laser RIN	−160 dB/Hz
Baud rate	56 Gbaud	PD responsibility	0.65 A/W
Tx bandwidth (3 dB)	25 GHz	PD dark current	10 nA
Rx bandwidth (3 dB)	35 GHz	PD thermal noise	20 pA/Hz
IL of 90° optical hybrid	1.2 dB	IL of coupler	0.15 dB
IL of polarizer	0.2 dB	IL of PBS	0.5 dB

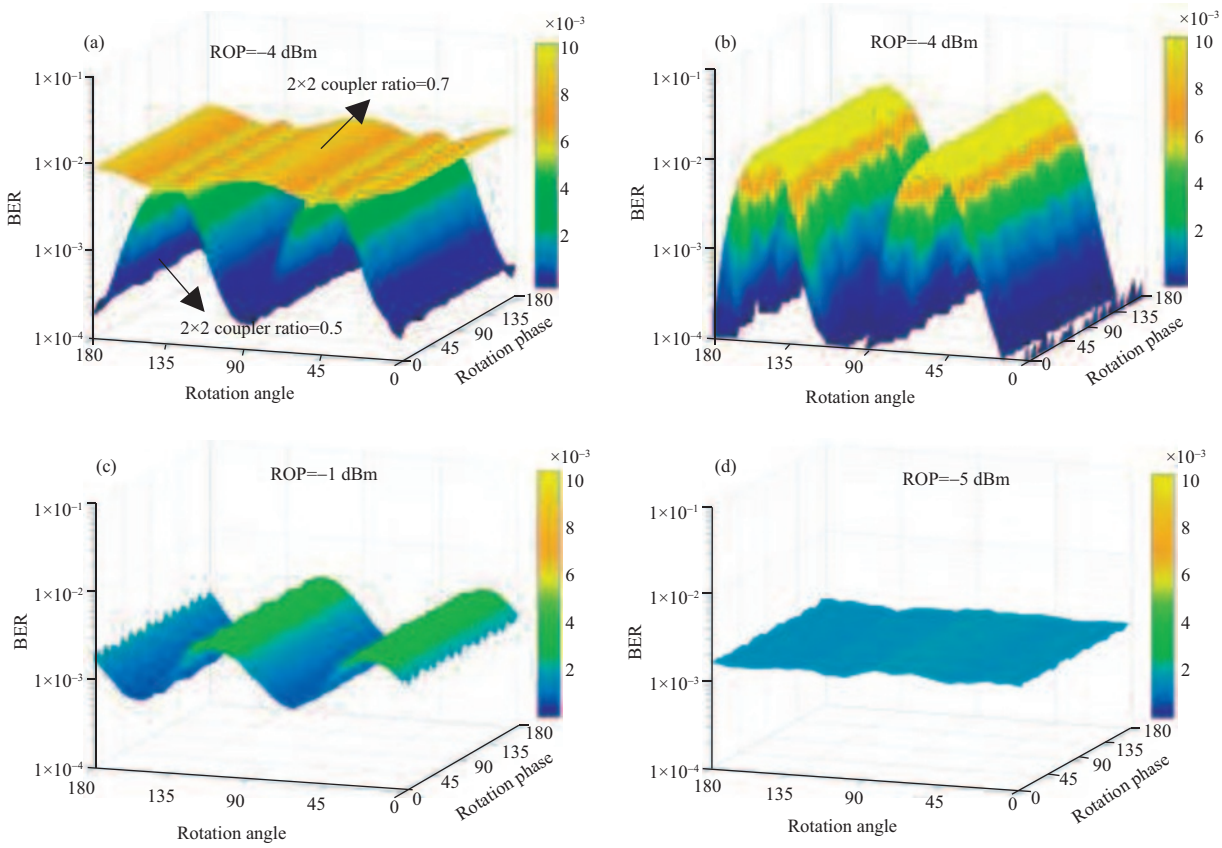

Figure 4 (Color online) BER performance as a function of the SOP angles for 224 Gbit/s PDM-PAM4 signal detection using different SVRs. (a) Receiver A, (b) receiver B, (c) receiver C, and (d) receiver D.

the intensity of two orthogonal polarization from a laser at a wavelength of 1310 nm and combined by a polarization beam combiner (PBC). After propagation through an optical fiber, a variable optical attenuator (VOA) is placed after the SSMF to adjust the received optical power (ROP). At the receiver side, the optical signals are detected by different SVRs. After an analog-to-digital converter (ADC), the detected digital signals are normalized and resampled to 2 samples per symbol. Mapping matrices are used to recover S_R. Then, adaptive equalization based on T/2-spaced FIR filters is used for polarization demultiplexing and equalization (De-Pol.& EQ). Finally, the BER is measured by bit error counting after the PAM4 decision and demapping. Table 1 summarizes the general settings of the simulation parameters based on commercial components.

In addition to the parameters mentioned above, we analyzed the impact of the SOP angle on the BER performance for various SVRs, and the result is shown in Figure 4(a)–(d). The ROPs are set to −4, −4, −1 and −5 dBm for receivers A–D, respectively. The SOP affects the system performance appropriately. The system performance becomes independent of the SOP when $\gamma = 0.7$ and $\gamma = 0.5$ for receivers A and D. We notice that BER fluctuation with the SOP angles matches the normalized noise power fluctuation

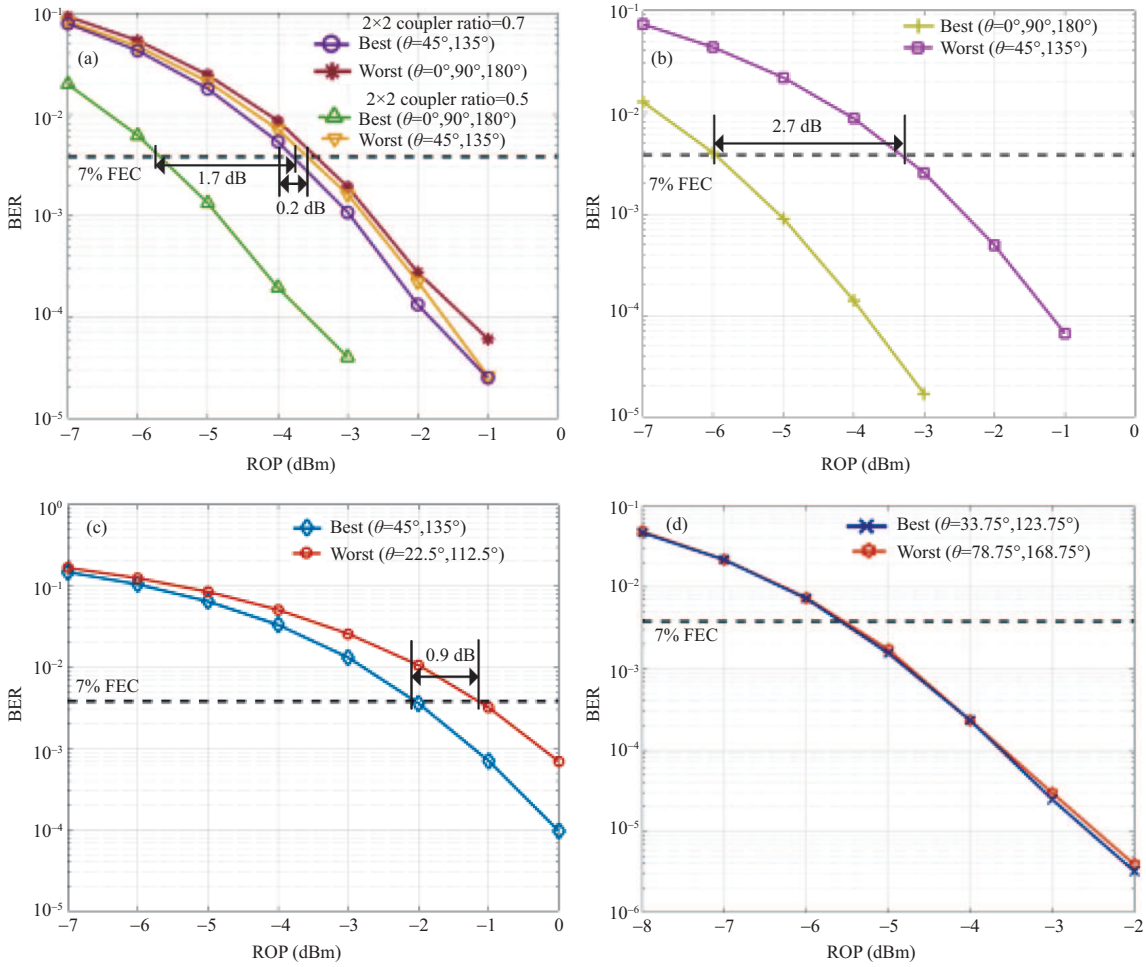

Figure 5 (Color online) Simulation results of the BER vs. ROP at the best and worst SOP angles for 224 Gbit/s PDM-PAM4 signals. (a) Receiver A, (b) receiver B, (c) receiver C, and (d) receiver D.

with the SOP angles.

The receiver noise power changes with the SOP rotation. The BER fluctuates for various SOP angles. We then extracted the BER vs. ROP performance for the worst and best SOP angles, and the results are shown in Figures 5(a)–(d). We observe an approximately 1.7 dB penalty between the worst and best SOP angles for receiver A with a 2×2 coupler ratio of $\gamma = 0.5$. This penalty gap between the worst/best SOP angles is closed when the 2×2 coupler ratio is $\gamma = 0.7$. For receiver B, the best SOP angles are $\theta = 0°, 90°, 180°$, and the worst SOP angles are $\theta = 45°, 135°$. The gap is as large as 2.7 dB. For receiver C, the overall noise power is high, the best SOP angles are $\theta = 45°, 135°$, and the worst SOP angles are $\theta = 22.5°, 112.5°$. The gap in the receiver sensitivity between the best/worst performance is 0.9 dB. For receiver D, the system performance is independent of the SOP angles.

Finally, we investigated the system performance of the four SVRs after 2 km transmission at C band. The accumulated CD is 34 ps/nm for 2 km SSMF. We measured the worst-case SOP angles at each ROP point, because in a real communication system, system performance is determined by worst-case scenarios. Figure 6 shows the measured BER as a function of the ROP for 224 Gbit/s PDM-PAM4 signals by using different SVRs. The receiver sensitivities at 7% over the head forward error correction (FEC) limit of 3.8E−3 are −3.5 dBm (receiver A, $\gamma = 0.5$), −3.2 dBm (receiver A, $\gamma = 0.7$), −2.8 dBm (receiver B), −0.8 dBm (receiver C) and −5.3 dBm (receiver D), respectively. Here, receiver D achieves the best performance.

Table 2 shows the comparison of different SVRs in terms of main devices, noise fluctuation, system performance variation and receiver sensitivity. Taken into account various performance attributes, we

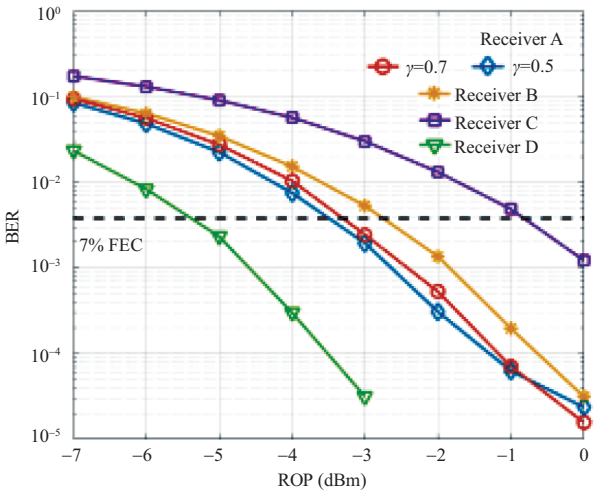

Figure 6 (Color online) Simulation results of 224 Gbit/s PDM-PAM4 signals after C band 2 km transmission for different SVRs.

Table 2 Comparison of 224 Gbit/s PDM-PAM4 signals with different SVRs

SVR scheme	Main devices	Noise fluctuation (@ different SOP)	System performance variation (@ fixed ROP) (dB)	Receiver sensitivity (@7% FEC) (dBm)
Receiver A $\frac{\gamma=0.5}{\gamma=0.7}$	1 hybrid+ 2 BPDs+2 PDs	Medium	1.7	−3.5
		Low	0.2	−3.2
Receiver B	1 hybrid+4 PDs	High	2.7	−2.8
Receiver C	1 wave plate+3 polarizers+4 PDs	Medium	0.9	−0.8
Receiver D	1 2×2 coupler +1 3×3 coupler+4 PDs	Low	0	−5.3

believe that receiver D is the best choice for high speed short-reach transmission as it is relatively simple with good performance. However, receiver D is still much more complex compared to single polarization IM-DD systems with higher cost and insertion loss, which directly translates into penalty on receiver sensitivity or optical signal-to-noise ratio (OSNR). Therefore, further investigations are needed to explore the tradeoffs between cost, hardware complexity, and spectral efficiency. To reduce SVR form factors and cost, system integration based on a single photonic integrated circuit (PIC) using either Silicon (Si), Indium Phosphide (InP) or a hybrid platform is a promising solution. This will reduce the insertion losses compared to using discrete components and will make the solution more viable for practical applications by lowering the cost, size and power consumption.

4 Conclusion

In this paper, we developed the PD thermal noise for PDM-IM-DD systems with different SVR architectures, i.e., a 90° optical hybrid with 2 BPDs and 2 PDs, a 90° optical hybrid with 2 PDs, a Stokes analyzer and a 3 × 3 coupler with 4 PDs. The corresponding demultiplexing matrix of the different SVR architectures is required to recover the Stokes vectors from the detected signals, which, combined with an arbitrary SOP, will change the effect of noise dynamically and significantly influence the system performance. We fairly evaluated these four SVRs via the PD thermal noise during the Stokes vector recovery. The relationship between the SOP and the PD thermal noise was studied in numerical simulations. To verify the theoretical analyses, a 224 Gbit/s PDM-PAM4-DD simulation setup was demonstrated. The BER performance for different SOPs was analyzed by using the normalized noise power. The simulation

results showed that the BER performance of the systems is consistent with the theoretical noise power variation curves. The receiver D based on a 3×3 coupler with 4 PDs outperformed the other three SVRs. This paper offers a theoretical analysis of a PDM-IM-DD system, which is helpful for the practical design of SVR-based systems.

Acknowledgements This work was supported by National Key Research and Development Program of China (Grant No. 2019YFB1803905), National Natural Science Foundation of China (Grant Nos. 61671053, 61871030), Fundamental Research Funds for the Central Universities (Grant No. FRF-TP-19-017A1), State Key Laboratory of Advanced Optical Communication Systems Networks, China, the Open Fund of IPOC (BUPT) (Grant No. IPOC2018B009), Foundation of Beijing Engineering and Technology Center for Convergence Networks and Ubiquitous Services, and Hong Kong Polytechnic University (Grant Nos. 1-ZVGB, G-SB65, 4-BCCK).

References

1 Zhong K P, Zhou X, Huo J H, et al. Digital signal processing for short-reach optical communications: a review of current technologies and future trends. J Lightwave Technol, 2018, 36: 377–400
2 El-Fiky E, Samani A, Patel D, et al. 400 Gb/s O-band silicon photonic transmitter for intra-datacenter optical interconnects. Opt Express, 2019, 27: 10258–10268
3 Li Z H, Shubin I, Zhou X. Optical interconnects: recent advances and future challenges. Opt Express, 2015, 23: 3717–3720
4 Zhou X, Urata R, Liu H. Beyond 1 Tb/s datacenter interconnect technology: challenges and solutions. In: Proceedings of Optical Fiber Communication Conference, 2019. Tu2F.5
5 Cheng J C, Xie C J, Chen Y Z, et al. Comparison of coherent and IMDD transceivers for intra datacenter optical interconnects. In: Proceedings of Optical Fiber Communication Conference, 2019
6 Che D, Li A, Chen X, et al. Rejuvenating direct modulation and direct detection for modern optical communications. Opt Commun, 2018, 409: 86–93
7 El-Fiky E, Samani A, Alam M S, et al. A 4-lane 400 Gb/s silicon photonic transceiver for intra-datacenter optical interconnects. In: Proceedings of Optical Fiber Communication Conference, 2019. Th3A.3
8 Huo J H, Zhou X, Zhong K P, et al. Transmitter and receiver DSP for 112 Gbit/s PAM-4 amplifier-less transmissions using 25G-class EML and APD. Opt Express, 2018, 26: 22673–22686
9 Zhang J, Yu J J, Zhao L, et al. Demonstration of 260-Gb/s single-lane EML-based PS-PAM-8 IM/DD for datacenter interconnects. In: Proceedings of Optical Fiber Communication Conference, 2019. W4l.4
10 Zhou J, Qiao Y J, Huang X C, et al. Joint FDE and MLSD algorithm for 56-Gbit/s optical FTN-PAM4 system using 10G-class optics. J Lightwave Technol, 2019, 37: 3343–3350
11 Che D, Shieh W. Achievable rate comparison between entropy and bit loading in a 100-Gb/s DM-DD DMT system. In: Proceedings of Optical Fiber Communication Conference, 2019. W1F.3
12 Tanaka T, Nishihara M, Takahara T, et al. Experimental demonstration of 448-Gbps+ DMT transmission over 30-km SMF. In: Proceedings of Optical Fiber Communication Conference, 2014. M2I-5
13 Olmedo M I, Zuo T J, Jensen J B, et al. Multiband carrierless amplitude phase modulation for high capacity optical data links. J Lightwave Technol, 2014, 32: 798–804
14 Tao L, Ji Y, Liu J, et al. Advanced modulation formats for short reach optical communication systems. IEEE Netw, 2013, 27: 6–13
15 Morsy-Osman M, Chagnon M, Poulin M, et al. 224-Gb/s 10-km transmission of PDM PAM-4 at 1.3 μm using a single intensity-modulated laser and a direct-detection MIMO DSP-based receiver. J Lightwave Technol, 2015, 33: 1417–1424
16 Kikuchi K. Electronic polarization-division demultiplexing based on digital signal processing in intensity-modulation direct-detection optical communication systems. Opt Express, 2014, 22: 1971–1980
17 Shieh W, Khodakarami H, Che D. Polarization diversity and modulation for highspeed optical communications. APL Photon, 2016, 1: 040801
18 Morsy-Osman M, Chagnon M, Plant D V. Four-dimensional modulation and stokes direct detection of polarization division multiplexed intensities, inter polarization phase and inter polarization differential phase. J Lightwave Technol, 2016, 34: 1585–1592
19 Che D, Yuan F, Shieh W. 200-Gb/s polarization-multiplexed DMT using stokes vector receiver with frequency-domain MIMO. In: Proceedings of Optical Fiber Communication Conference, 2016. Tu3D.4
20 Pan Y, Yan L S, Yi A L, et al. Simplified demultiplexing scheme for two PDM-IM/DD systems utilizing a single Stokes analyzer over 25-km SMF. Opt Lett, 2017, 42: 4071–4074
21 Chagnon M, Morsy-Osman M, Plant D V. Half-terabit single-carrier direct-detect transceiver, formats, and DSP: analysis and demonstration. J Lightwave Technol, 2017, 36: 447–459
22 van den Borne D. Robust optical transmission systems: modulation and equalization. Dissertation for Ph.D. Degree. Eindhoven: Eindhoven University of Technology, 2008
23 Chen C-L. Elements of Optoelectronics and Fiber Optics. New York: McGraw-Hill, 1996